INVESTIGATION OF CATTLE BIRTH SEASONALITY USING $\delta^{13}C$ AND $\delta^{18}O$ PROFILES WITHIN FIRST MOLAR ENAMEL

Jacqueline Towers [1*], Andrew Gledhill [1], Julie Bond [1] and Janet Montgomery [2]

[1] Division of Archaeological and Environmental Sciences, University of Bradford, Bradford, UK BD7 1DP.

[2] Department of Archaeology, University of Durham, South Road, Durham, UK DH1 3LE.

[*] Corresponding author – J.R.Towers@student.bradford.ac.uk.

ABSTRACT

Cattle (*Bos Taurus*) are biologically able to breed year-round, potentially giving farmers the freedom to choose a calving strategy to best meet their economic goals. Thus, an accurate method to determine cattle birth seasonality from archaeological remains would prove a valuable tool when investigating a prehistoric farming community. This paper presents the results of intra-tooth isotope ratio analysis ($\delta^{18}O$, $\delta^{13}C$) of first, second and third molars from 15 cattle. The principal outcome is a possible new approach to determine cattle birth seasonality utilising both carbon and oxygen isotope ratio measurements of first molar enamel. Although this technique requires verification through more extensive testing, particularly of modern material, initial results suggest that it may produce more accurate predictions of birth seasonality than techniques based on intra-tooth $\delta^{18}O$ measurements of second and third molars.

KEYWORDS: TOOTH ENAMEL, MOLAR FORMATION, CATTLE, BIRTH SEASONALITY, OXYGEN, CARBON, ISOTOPE RATIO ANALYSIS

INTRODUCTION

The ability to detect past animal husbandry practices is essential if the economic basis of a prehistoric community is to be understood. One aspect of animal husbandry, seasonality of birth, is of particular importance when determining the role of domestic cattle (*Bos Taurus*) within a community. Cattle are biologically able to mate and breed year-round (King 1978, 124), potentially giving farmers the freedom to choose a calving strategy to best meet their economic goals, whether for an emphasis on milk or meat. For example, before the advent of specialised, modern, dairy breeds, a year-round supply of fresh milk is likely to have required calving over several seasons. An accurate method to determine cattle birth seasonality from archaeological remains would provide valuable information on both economic focus and the management effort required to achieve a particular calving strategy.

Oxygen isotope ratio analysis of molar enamel is increasingly being used to investigate birth seasonality of domestic herbivores (e.g. Balasse *et al.* 2003; Balasse and Tresset 2007; Henton *et al.* 2010; Blaise and Balasse 2011; Stevens *et al.* 2011; Towers *et al.* 2011; Balasse *et al.* 2012a; Balasse *et al.* 2012b). This technique appears ideally suited to this application for two principal reasons. First, the molar teeth of many herbivorous mammals are high-crowned (hypsodont), each molar forming sequentially over a period of time from the cusp at the occlusal surface to the cervix, where the root and crown meet (Brown *et al.* 1960; Hillson 2005, 8-15). Second, the isotopic ratio of the oxygen incorporated into enamel during its formation tends to vary seasonally. Thus, by analysing a series of intra-tooth enamel samples extracted along the length of a molar crown from cusp to cervix, the seasonal variation in oxygen isotope ratio can be revealed (Fricke and O'Neil 1996). For cattle that have lived at mid- and high latitudes, the form of this variation generally follows a sinusoidal-like pattern

with minima corresponding to winter and maxima to summer (Fricke *et al.* 1998). By comparing the positioning of minima or maxima within the second or third molars of a number of cattle present in an archaeological assemblage, seasonality of birth, i.e. whether calving was restricted to a narrow time period or spread across a number of seasons, may be estimated.

However, the use of this technique for assessing cattle birth seasonality (referred to here as method 1) relies on a series of assumptions principally related to molar crown formation both in terms of chronology and rate of growth. Inter-animal and intra-tooth variability in crown formation are not well understood and, if present, will introduce a degree of uncertainty into any estimates of birth seasonality based on assumptions of uniformity. A method to correct for inter-animal variability in molar growth rate by modelling the sinusoidal pattern and normalising to period has been proposed by Balasse *et al.* (2012a). The initial aim of the present study was to identify and attempt to quantify the principal sources of uncertainty. The approach was to obtain intra-tooth oxygen isotope data from first, second and third molars of a number of cattle from various archaeological sites in the British Isles. Combined plots of oxygen isotope ratio versus time were constructed by applying a common set of assumptions related to crown formation. The isotopic analysis carried out in this study was of the carbonate fraction of enamel bioapatite, resulting in both oxygen and carbon isotope ratios being measured concurrently. An unforeseen consequence of this analysis has been the identification of a possible new method for estimating cattle birth seasonality (method 2) based on how the carbon isotope ratio varies along the length of the first molar crown and its relationship to the seasonal patterning of the oxygen isotope ratio also recorded in the crown. Although both carbon and oxygen isotope ratio data will be affected by variability in the timing and rate of crown formation, direct comparison between the two isotope patterns

removes these sources of uncertainty from any estimate of birth seasonality. Hence, method 2 has the advantage that it does not rely on detailed knowledge of molar formation.

BACKGROUND

Cattle molar crown formation

Although cattle molar crown formation can be described simplistically as sequential, progressing from the cusp to the cervix over a period of several months, the actual process is much more complex. By means of detailed radiographic and optical examination of hypsodont molars from goats and sheep, Suga (1982) concluded that enamel mineralization follows two principal phases: matrix deposition and maturation. The matrix is essentially an organic structure acting as a framework for the ensuing maturation process. It is secreted from cusp to cervix and becomes lightly mineralized as it is deposited (Hillson 2005, 155). As the matrix front progresses, with a periodicity revealed through incremental structures known as the brown striae of Retzius (Hillson 2005, 161), the enamel begins to mature but only after the matrix has reached its final thickness (Suga 1982). Most of the mineralization occurs during the maturation phase (Robinson *et al.* 1995), which, in contrast to the relatively simple progression of matrix deposition, is a complex process both spatially and temporally (Suga *et al.* 1979; Suga 1982; Hoppe *et al.* 2004; Tafforeau *et al.* 2007). Suga (1982) proposed three phases to the maturation process: an initial increase in mineralization from the surface to the innermost layer, followed by a second increase in the reverse direction, and finally an increase in mineralization of a narrow subsurface layer. Consequently, cattle molar enamel at any position on the crown takes at least 6-7 months to complete mineralization (Balasse 2002; Zazzo *et al.* 2005; Montgomery *et al.* 2010). It is also possible that the total length of time

required for enamel mineralization is variable within a single tooth, as observed in deciduous bovine incisors (Deutsch *et al.* 1979), and between different teeth of similar crown heights, as observed in equine premolars and molars (Hoppe *et al.* 2004).

A chronology of molar development has been determined for modern cattle by Brown *et al.* (1960) through radiography (Table 1). However, these timings do not take account of the maturation process and are related to the progression of the matrix. There is uncertainty in the start and finish times, since, in addition to being displayed as ranges, they are described by Brown *et al.* (1960) as "approximations". Detailed studies of molars from other bovids (sheep, goats and the extinct *Myotragus balearicus*) report a reduction in the rate of matrix progression towards the cervix with approximately 75 % of the crown length being formed during the first half of the formation period (Jordana and Köhler 2011; Kierdorf *et al.* 2012; Zazzo *et al.* 2012). However, according to Hillson (2005, 163), the striae of Retzius in cattle teeth, viewed at the enamel surface as troughs known as perikymata, tend to be regularly spaced along "most of the crown height" suggesting a reasonably constant rate of matrix progression for much of the crown.

Stable isotope ratio analysis of cattle molar enamel

Isotope ratio analysis of the carbonate fraction of enamel bioapatite (the mineral component of enamel) enables both oxygen and carbon isotope ratios to be measured concurrently. Isotope ratios are expressed as $\delta^{18}O$ and $\delta^{13}C$ and units are per mil (‰) (Sharp 2007, 17-18). The $\delta^{18}O$ values measured in bioapatite are primarily controlled by the $\delta^{18}O$ value of ingested drinking water which is usually related to that of precipitation (Longinelli 1984; Luz *et al.* 1984; Luz and Kolodny 1985). The $\delta^{18}O$ value of precipitation varies seasonally due to a

range of climatic variables including the amount of precipitation and air temperature (Dansgaard 1964) and, at mid- to high latitudes, it tends to be more positive in summer. Because of the averaging effect resulting from the lengthy mineralization process of enamel, the pattern of $\delta^{18}O$ recorded along the length of a hypsodont molar crown (its intra-tooth $\delta^{18}O$ profile) is damped and temporally shifted relative to the input $\delta^{18}O$ signal (Passey and Cerling 2002; Kohn 2004). It generally follows a sinusoidal-like form with maxima corresponding to summer and minima to winter (Fricke *et al.* 1998). It is the positioning of this sinusoidal pattern within a molar crown that, through comparison between different animals, forms the basis of method 1 estimates of birth seasonality. If the time taken for enamel mineralization were variable along the length of a molar crown then the amount of damping and temporal shift would also be variable, leading to possible distortions in the recorded sinusoidal pattern. As a result, errors would be introduced into method 1 estimates of birth seasonality in addition to those errors arising from any variation in crown formation start and finish times and the rate of matrix deposition.

For herbivores, the $\delta^{13}C$ values measured in bioapatite are controlled by diet (Sullivan and Krueger 1981). In prehistory, the indigenous terrestrial vegetation of the British Isles together with any crops available for fodder would have photosynthesized by the C_3 pathway. Therefore, $\delta^{13}C$ values measured in prehistoric cattle enamel are expected to reflect a C_3-based diet. However, interpretation of diet is not an aim of this study. Instead it is the intra-tooth $\delta^{13}C$ profile of first molar enamel that is of particular interest. Other studies have shown a distinctive pattern within the first molar $\delta^{13}C$ data of cattle (Balasse 2002) and sheep (Towers and Montgomery, unpublished data): moving from earlier forming enamel at the cusp towards later forming enamel at the cervix, first molar $\delta^{13}C$ profiles tend to start at relatively low levels, rise steeply, then level off or show a reduction in gradient to values

more typical of second molar enamel. In terms of matrix progression, a first molar crown starts forming several months before birth and is complete when the calf is approximately 2-3 months old (Table 1). Consequently, the first molar crown forms during the key stages in a calf's digestive development (described below), and the $\delta^{13}C$ profile recorded in the tooth is likely to reflect this.

The source of carbon in enamel is dissolved inorganic carbon in the bloodstream (Sullivan and Krueger 1981). In a ruminant, the fermentation of food is brought about by micro-organisms in the rumen, the first of four stomach compartments, which produces both carbon dioxide and methane (McDonald *et al.* 1988, 142-143). The $\delta^{13}C$ value of the methane is much more negative than the food, by more than 30 ‰ (Rust 1981; Metges *et al.* 1990; Schulze *et al.* 1997) whilst the carbon dioxide becomes enriched in ^{13}C (Hedges 2003). Thus, if a proportion of this carbon dioxide becomes dissolved in the bloodstream, the $\delta^{13}C$ value of any mineralizing enamel is expected to be more positive than for a non-ruminant herbivore with a comparable diet (Cerling and Harris 1999; Passey *et al.* 2005). When the first molar begins forming, the dissolved carbon in the foetal calf's blood is derived from its mother's digestion processes. Hence, the $\delta^{13}C$ value of forming enamel will be typical of a ruminant. When the calf is born, its rumen is undeveloped and digestion of milk is carried out in the abomasum, the fourth stomach compartment in a ruminant, which digests food in a similar manner to the stomach of a non-ruminant. Therefore, immediately after birth, the $\delta^{13}C$ value of forming enamel is expected to be typical of a non-ruminant; i.e. more negative. However, given the opportunity, young calves will begin to consume some solid food by the age of 2 weeks (Lengemann and Allen 1959; Godfrey 1961a). It is the consumption of dry food that stimulates the development of the rumen. Provided such food is available, the rumen develops quickly, anatomically, physiologically and microbially, so that by the time the calf is

approximately 6-10 weeks old, it is able to digest solid food as an adult ruminant (Bryant *et al.* 1958; Swanson and Harris 1958; Godfrey 1961b; Anderson *et al.* 1987). Thus, from this age, the $\delta^{13}C$ value of forming enamel will be more typical of a ruminant even though the calf may not be fully weaned.

Transition of the calf from ruminant (via its mother) through non-ruminant and back to ruminant might be expected to produce relatively higher $\delta^{13}C$ values in the earliest and latest forming enamel of an *unworn* first molar and lower values between. However, most analysed first molars are worn. Because enamel mineralization takes several months (Balasse 2002) and since, according to Brown *et al.* (1960), only one third of the crown is formed at birth, any enamel that started forming before birth is likely to be worn away or, if remaining, produce a $\delta^{13}C$ value predominantly reflecting post-birth digestion. If a rise in $\delta^{13}C$ towards the cervix is observed in first molars, then this may indicate the transition between non-ruminant digestion immediately after birth and the utilisation of a fully formed rumen several weeks later. Equally, a reduction in gradient of the $\delta^{13}C$ profile to values more typical of second molar enamel may be a direct indication of the completion of rumen functionality and, consequently, an indirect indication of birth recorded within the isotopic data. If this is the case, this feature has the potential to provide an alternative method to estimate cattle birth seasonality (method 2).

MATERIALS AND METHODS

Thirty five archaeological mandibular molars from 13 different cattle were selected from three archaeological assemblages: Pool, Orkney, UK (Scandinavian Interface period, c. A.D. 800 – c. A.D. 950); Mine Howe, Orkney, UK (Iron Age period, c. A.D. 100 – c. A.D. 400);

and Grimes Graves, Norfolk, UK (Middle Bronze Age period, c. 1100 B.C.) (Mercer 1981, 36; Hunter 2007, 140; Davis 2010, 417). For nine of these animals, first, second and third molars were analysed whilst, for the remaining four, first and second molars were analysed. For each site, care was taken to ensure that the molar series were from different individuals; i.e. if two series of molars were from opposite sides of the mouth, they had to be distinguishable visually in terms of wear or isotopically after analysis. In addition, first molars and fourth deciduous premolars were analysed for two modern animals: one cow from the Chillingham Wild White Cattle herd, Northumberland, UK (Hall 1989) and one Dexter bull reared for beef in County Durham, UK.

Before intra-tooth enamel sampling could proceed, each cattle tooth was prepared by cleaning the enamel surface of a single lobe using a diamond dental burr. For the archaeological molars, lingual mesial lobes were targeted unless the enamel appeared of poorer quality than that of alternative lobes. For three animals, lingual distal lobes for second molars and lingual central lobes for third molars were sampled. Lingual mesial and distal/central lobes are very similar in terms of length and enamel thickness, and it is assumed that estimates of the timings of $\delta^{18}O$ minima and maxima will also be very similar. Powdered enamel samples were obtained from along the length of the lobe, using a clean diamond dental burr, such that the drilling of each sample, through the bulk of the enamel thickness, produced a groove approximately 2 mm wide perpendicular to the lobe length. Further processing followed a protocol modified after Sponheimer (1999) for finely powdered enamel, involving initial treatment with 1.7% NaOCl solution (for approximately 30 minutes) to remove organic matter. After rinsing with de-ionised water they were then treated with 0.1M acetic acid (for < 10 minutes) to remove any exogenous carbonate. After further rinsing followed by freeze-drying, the samples were weighed into septa-capped vials (~ 1.3 mg for each sample), which

were loaded into a Finnigan Gasbench II, an automatic carbonate preparation device connected to a Thermo Delta V Advantage continuous flow isotope ratio mass spectrometer. The carbonate fraction of each sample reacted with phosphoric acid (103%) at 70 °C to release CO_2 which was analysed by the mass spectrometer. $\delta^{18}O_{VSMOW}$ and $\delta^{13}C_{VPDB}$ measurements were normalised using a calibration equation derived from the measured and accepted values of one international and two internal standards. Analytical precision was ± 0.2‰ for $\delta^{18}O_{VSMOW}$ (1σ) and ± 0.1‰ for $\delta^{13}C_{VPDB}$ (1σ), determined from repeated analyses of an internal enamel laboratory standard (n = 33 over 15 months). Sampling and analysis was carried out at the Stable Light Isotope Facility at the University of Bradford.

RESULTS AND DISCUSSION

Oxygen and carbon isotope results are shown in Table 2. They were obtained from the molars of 5 Pool animals (PL0278, PL0330, PL0339, PL0344 and PL0386), 3 Mine Howe animals (MH84, MH138 and MH0604), 5 Grimes Graves animals (GG120, GG743, GG839, GG614 and GGT10), the modern Chillingham animal (CHIL1) and Dexter (KAR).

Construction of $\delta^{18}O$ and $\delta^{13}C$ profiles

In order to assess the timing and uniformity of cattle molar formation, it is necessary to plot intra-tooth oxygen and carbon isotope ratios versus time rather than the distance from cervix measurements in Table 2. Because the only timing information available relates to the start and finish times of each molar (Brown *et al.* 1960), conversion of distance from cervix to time requires unworn crown heights. In many cases, these must be predicted because the molars are worn.

For all 13 archaeological cattle, the data for first, second and third molars, where present, have been combined onto the same plot. The resulting isotopic profiles are shown in Figure 1 and were produced as follows:

1) Unworn crown heights were predicted for worn third molars from graphs of wear stage versus crown height constructed using measurements of 46 third molars from Mine Howe (wear stage data from Davis 2010, Appendix V, wear stage classification from Grant 1982). The graphs provide incremental corrections for each wear stage in mm depending on which enamel lobe is being sampled (Predicted crown heights_SuppInfo.doc). The incremental corrections for the lingual mesial lobe are 0, 0.9, 2.1, 3.7, 5.6 and 7.9 mm for wear stage a-f respectively. Those for the lingual central lobe are 0, 0.6, 1.7, 3.2, 5.1 and 7.3 mm. Each predicted unworn crown height was obtained by adding the appropriate incremental correction to the worn crown height. For this study, only third molars with wear stages a-f were used because wear stages g-m depend on the accessory pillar height which can vary substantially between animals (Jones 2007), introducing more uncertainty to the wear stage correction. Despite being derived from Mine Howe molars, the incremental corrections have been used for all Mine Howe, Pool and Grimes Graves third molars since, whatever the original size of the unworn tooth, any difference between the actual and predicted amounts of wear will be relatively small, translating to an equally small error in the predicted unworn molar size. For animals where only first and second molars were analysed, the similar size and morphology of second and third molars allowed unworn crown heights for second molars to be predicted using the third molar correction factors for wear stages a-f.

2) For each molar series that includes a third molar, the unworn second molar crown height was calculated to be 97 % of the predicted unworn crown height of the third molar. The figure

of 97 % falls between a value closer to 100 % suggested by the limited examples available to this study and a figure of 94% suggested by Jones (2007).

3) Unworn first molar crown heights were calculated to be 84 % of the predicted unworn second molar crown heights. The figure of 84 % is suggested by Legge (1992, 21) for Grimes Graves cattle molars.

4) For each molar, the timing of each intra-tooth enamel sample relative to the cervix was calculated proportionally from the measured or calculated unworn crown height and the length of time the molar takes to form given by the chronology of Brown *et al.* (1960) (Table 1). The time after birth for each intra-tooth sample could then be calculated from the time after birth of the cervix given by the chronology. For these calculations, the start and finish times relative to birth were assumed to be –4.7 and 2.5 months for first molars, 1 and 12.5 months for second molars and 10 and 23.5 months for third molars. These are the mid-range times given by Brown *et al.* (1960) (Table 1) apart from the start time of 10 months for third molars, which was chosen because a start time of 9.5 months can produce visible misalignment between the profiles of second and third molars.

It should be emphasized that for each intra-tooth data point represented in the profiles of Figure 1, the time calculated using parameters from Brown *et al.* (1960) (x-axis value) is related to the initial deposition of the enamel matrix, whereas its measured isotopic ratio (y-axis value) is an average value of the completed enamel which took several subsequent months to mineralize following matrix deposition. The use of this method assumes that the crown formation times derived for modern teeth can be applied to archaeological teeth and that the matrix progresses at a uniform rate which is not true for first molars if only one third of the first molar crown is formed at birth (Brown *et al.*1960); i.e. the cuspal third forms before birth over a period of approximately 4.5 months and the remaining two thirds over a

shorter period of approximately 2.5 months. Although the first molar isotopic data have been plotted in Figure 1 according to calculations outlined in (4) above, the x-axis time scale has been removed for times before 2 months because of the non-uniformity of first molar matrix progression.

Second and third molar $\delta^{18}O$ profiles: the basis for method 1 estimates of cattle birth seasonality

The assumptions used in the construction of isotope ratio profiles appear to have resulted in profiles that are continuous both in $\delta^{18}O$ and $\delta^{13}C$ and show little evidence of obvious discontinuity between molars (Fig. 1). In each profile, the seasonal, sinusoidal-like variation in $\delta^{18}O$ is clearly visible. Generally, there is a minimum present in the second molar $\delta^{18}O$ profile (or straddling the first and second molar profiles), a second minimum present in the third molar $\delta^{18}O$ profile and a maximum falling between. The timing of each of these minima and maxima has been calculated by differentiation of a second order polynomial fitted to the surrounding data points. Timings for all 13 cattle are presented in Table 3. These timings will have an uncertainty associated with them, arising from the assumptions made when constructing the $\delta^{18}O$ profiles. For third molars, there is an error associated with the predicted unworn crown height, derived from the measurement of the worn crown height and the incremental correction derived for each wear stage. Worst case errors of ± 1.0 mm (2σ) and ± 2.5 mm (2σ) respectively are estimated, resulting in a combined error of $\pm \sqrt{(0.5^2 + 1.25^2)} =$ ± 1.35 mm (1σ), using the sum of squares method for combining independent errors (Berendsen 2011, 21). For a typical unworn third molar crown of height 50 mm and formation time 13.5 months, this translates into an error of ± (1.35/50) x 13.5 = ± 0.36 months (1σ). For second molars, the predicted unworn crown height is calculated as 97 % of the

predicted unworn crown height of the third molar, and its associated error is a combination of the errors associated with the third molar unworn crown height and the scaling factor of 97 %. Suggested percentage errors are ± 3 % (1σ) and ± 1.5 % (1σ) respectively, resulting in a combined percentage error of ± $\sqrt{(3^2 + 1.5^2)}$ = ± 3.4 % (1σ) (Berendsen 2011, 21). For a second molar formation time of 11.5 months, this translates into an error of ± 0.034 x 11.5 = ± 0.39 months (1σ). These timing errors are modest but do not include contributions arising from variation in crown formation in terms of start and finish times or intra-tooth variability.

Table 3 also includes values for the differences in timing between neighbouring maxima and minima, [max – min 1] and [min 2 – max]. These values vary from animal to animal. Although inter-animal difference in molar crown formation may be a contributing factor, another is likely to be the variation in the enamel's $\delta^{18}O$ *input* signal during formation. For example, if a 7 month rolling average (a crude approximation to the averaging process occurring during enamel formation) is applied to monthly precipitation $\delta^{18}O$ data from Wallingford, UK (Darling and Talbot 2003), the resulting summer maxima and winter minima (not shown) are not always exactly 6 months apart. In contrast, the *mean* separation between neighbouring minima and maxima is expected to be 6 months. This is true for the precipitation $\delta^{18}O$ data from Wallingford (Darling and Talbot 2003) for which the mean separation between neighbouring minima and maxima is 6.0 ± 1.0 months (1σ) over a 14 year period. For the molars in this study, the mean value of [max – min 1] = 5.5 ± 0.4 months (1σ, n = 11) and the mean value of [min 2 – max] = 6.3 ± 0.9 months (1σ, n = 9). This difference may be a manifestation of the small sample size. Alternatively, it may indicate that the chronology of second and third molars used here is not optimal. It is possible to obtain mean values of [max – min 1] and [min 2 – max] that are close to 6 months by adjusting the start and finish times relative to birth to 0.5 and 13.5 months for second molars (rather than 1 and

12.5 months) and to 11 and 23 months for third molars (rather than 10 and 23.5). None of these revised parameters falls more than one month outside the ranges given by Brown *et al.* (1960) for modern molars. Such discrepancies may reflect the approximate nature of those ranges or the fact that the molars are not from modern animals. The original parameters will be used for the remainder of this study since both sets of parameters produce the same overall conclusions.

First molar $\delta^{13}C$ and $\delta^{18}O$ profiles: the basis for method 2 estimates of cattle birth seasonality

In order to gauge the magnitudes of the errors involved in any method 1 estimate of cattle birth seasonality derived from $\delta^{18}O$ minima and maxima, an alternative method is required for comparative purposes. Method 2 makes use of the shape of the $\delta^{13}C$ profile recorded in first molar enamel: moving towards the cervix, there is a steep increase in first molar carbon isotope ratios followed by a reduction in gradient to values more typical of second molar enamel, patterning that is evident in the plots in Figure 1. As discussed, this patterning may indicate the transition between purely non-ruminant digestion immediately after birth (relatively low $\delta^{13}C$ values) and the utilisation of a fully formed rumen (relatively high $\delta^{13}C$ values), with the reduction in gradient indicating the completion of rumen functionality at the age of approximately 6-10 weeks. Figure 2a is a plot of $\delta^{13}C$ versus the distance from the cervix for the first molar and fourth deciduous premolar of the modern Dexter (KAR). The first molar $\delta^{18}O$ profile is also shown. Like the plots in Figure 1, the $\delta^{13}C$ profile of the Dexter's first molar shows an increase in $\delta^{13}C$ moving towards the cervix, followed by a reduction in gradient. Moving away from the cervix, the $\delta^{13}C$ profile passes through a minimum and begins to rise again in the cuspal enamel. This earliest-forming enamel may be reflecting foetal incorporation of ^{13}C-rich carbon resulting from the mother's ruminal

digestion. A similar pattern can be seen in the plot for GG120 (Fig. 1). Because the crown of a cattle fourth deciduous premolar is almost fully mineralized by the time of birth (personal observation), the $\delta^{13}C$ values recorded in the enamel of this tooth should be dominated by the mother's ruminal digestion. The plot in Figure 2a shows that the $\delta^{13}C$ values of the modern Dexter's fourth deciduous premolar enamel are similar to those recorded in its cervical first molar enamel. Plots for the same two teeth from the Chillingham animal (CHIL1) show an equivalent pattern (Fig. 2b). Thus, together, the fourth deciduous premolar and the first molar do appear to show the three stages in a calf's digestive development from ruminant (via its mother) through non-ruminant to ruminant.

If the change in gradient of the first molar $\delta^{13}C$ profile is an indication of the completion of rumen functionality and an indirect indication of birth, the relationship between it and the seasonal cycle of the $\delta^{18}O$ profile is of particular relevance. This relationship is critical to estimating cattle birth seasonality using method 2. For each animal represented in Figure 1, the data point where the $\delta^{13}C$ profile changes gradient, designated here as $\delta^{13}C_{CG}$, is indicated on the plot, as is the equivalent point in the $\delta^{18}O$ profile. The latter, $\delta^{18}O_{CG}$, has been assigned an angle relative to its position along the sinusoidal profile, A_{CG}, which is shown schematically in Figure 3a. This was achieved as follows: the magnitudes of the summer maximum and winter minimum, $\delta^{18}O_{max}$ and $\delta^{18}O_{min}$, bracketing the data point $\delta^{18}O_{CG}$ were calculated by differentiation of second order polynomials fitted to the surrounding data points (occasionally, when a maximum or minimum was not clearly defined, as for MH138, values had to be estimated by visual inspection). Angle A_{CG} was calculated using the equation $[\delta^{18}O_{CG} - \delta^{18}O_{min}] = 0.5\Delta[\cos(A_{CG}) + 1]$, where $\Delta = [\delta^{18}O_{max} - \delta^{18}O_{min}]$, and $[\delta^{18}O_{CG} - \delta^{18}O_{min}]$ lies between 0 and Δ (Fig. 3a). Angles A_{CG} calculated for all of the cattle in this study are presented in Table 4 and Figure 3b. Each angle A_{CG} will be subject to uncertainty. One source

of error arises from the identification of the data point $\delta^{13}C_{CG}$ in the $\delta^{13}C$ profile and, from that, its equivalent in the $\delta^{18}O$ profile, $\delta^{18}O_{CG}$. This was done by visual inspection which in some cases could have led to $\delta^{13}C_{CG}$ being assigned to the wrong data point. In this study, data points are separated by approximately 20° (corresponding to nine data points between neighbouring maxima and minima in the $\delta^{18}O$ profile). If the maximum error is ±1 data point, the error in A_{CG} is ± 20° (2σ). There are cases where the $\delta^{18}O$ maximum or minimum is not clearly defined, e.g. MH138 (Fig. 1) resulting in additional uncertainty in A_{CG}. This has been estimated to be approximately ± 20° (2σ). Using the sum of squares method for combining independent errors, the total error associated with A_{CG} becomes $\pm \sqrt{(10^2 + 10^2)} = \pm 14.1°$ (1σ) which, since 360° represents 12 months, is equivalent to ± 0.47 months (1σ).

It is proposed that birth seasonality for an archaeological assemblage, i.e. the spread of births throughout the year, may be estimated from the spread of angles A_{CG}, bringing into play a further source of error. If the change in gradient of the $\delta^{13}C$ profile, $\delta^{13}C_{CG}$, is an indication of the completion of rumen functionality, there will be variability in the timing of this biological event relative to birth. According to a number of studies (Bryant *et al.* 1958; Swanson and Harris 1958; Godfrey 1961b; Anderson *et al.* 1987), completion usually occurs at the age of approximately 6-10 weeks (8 ± 2 weeks), provided the calf has access to some dry food. If an estimate of ± 0.75 months (2σ) is assumed, the total error associated with the timing of birth is calculated to be $\pm \sqrt{(0.47^2 + 0.375^2)} = \pm 0.60$ months (1σ), incorporating the error in estimating A_{CG}.

Comparison of method 1 and method 2

The second molar $\delta^{18}O$ minima timings in Table 3 have been plotted against the angles in Table 4. The resulting plot is shown in Figure 4a. It might be expected that the data points should approximate to a straight line of gradient –12/360 months/°. Therefore, a straight line, of the form y = -(12/360)x + c, also shown in Figure 4a, has been fitted by adjusting the value of intercept c such that the sum of the squares of the residuals in the y direction is minimal. There is a strong correlation between angle A_{CG} and the timings of second molar $\delta^{18}O$ minima, supporting the idea that both types of data are related to the same factor, the timing of birth. The correlation coefficient r = -0.85 and the standard deviation of the residuals in the y direction, sd_{yres} = ± 1.2 months. Figure 4b shows an equivalent plot for the third molar $\delta^{18}O$ minima. In this case, the correlation coefficient r = -0.72 and sd_{yres} = ± 2.0 months.

Although the values of sd_{yres} for both types of molar will incorporate the annual climate-related variability in the $\delta^{18}O$ input signal and the errors associated with the construction of the $\delta^{18}O$ profiles, particularly the prediction of unworn crown heights, inter-animal variability in crown formation is likely to be a factor. This may arise from inter-animal differences in crown start and finish times as defined by the matrix deposition process and the time taken to complete enamel mineralization. Intra-tooth differences between animals in terms of varying rates of enamel matrix formation or maturation along the crown may also be contributing factors, although modelling of cattle third molars by Balasse *et al.* (2012b) suggests that intra-tooth variation may be insignificant. Variability in third molar crown formation appears to be much more pronounced than that of second molars, which is not altogether surprising since a similar trend has been observed in modern sheep second and third molars (Blaise and Balasse 2011). The timing of third molar formation in humans is also

highly variable (Hillson 1996, 136). It might be expected that the values of sd_{yres} would be improved through the modelling and normalisation technique proposed by Balasse et al. (2012a). However, this does not appear to be borne out in practice for these datasets. While the technique may correct for variation in the duration of crown formation, it does not address variability relative to birth of the start and finish times of crown formation. The advantage of method 2 is that it should be unaffected by variability in the timing and rate of molar formation. However, its predicted degree of uncertainty (± 0.6 months) cannot be accepted with confidence until the molars of many more cattle have been analysed, particularly from modern animals with known histories, and the associated uncertainties investigated and evaluated thoroughly. There may be sources of error not yet accounted for. For example, there may be an additional contribution to the uncertainty in A_{CG} due to distortion of the sinusoidal pattern of the first molar $\delta^{18}O$ profile caused by pre-weaning ingestion of water via milk, which tends to produce more elevated $\delta^{18}O$ values than drinking water (Lin *et al.* 2003; Renou *et al.* 2004; Camin *et al.* 2008).

As an illustration of how estimates of birth seasonality can depend on the method used, suppose that the animals included in this study were from the same herd and consider those data points in Figures 4a and 4b falling in the central cluster between angles -13° and +91°. The spread of births estimated using method 2 is (104/360) x 12 = 3.5 months. Alternatively, using method 1 and reading along the y-axes of Figures 4a and 4b, the spread of births is 8.6 - 3.4 = 5.2 months for second molars and 21.9 – 14.5 = 7.4 months for third molars. Thus, applying method 1 to third molars could lead to very different conclusions regarding cattle husbandry and economic goals than using method 2. If method 2 proves to be more accurate, then applying method 1 to third molars in particular could lead to erroneous conclusions,

which would be unfortunate as loose third molars are often the most common component in archaeozoological dental collections because they are easy to identify.

Estimating season of birth

The emphasis of this paper has been on the seasonality of births, i.e. the spread of births throughout the year. However, an ability to estimate the actual season of birth for an animal would contribute greatly to our understanding of past husbandry practices. In order to predict the season of birth using method 2, the analysis of molars from an animal with a known date of birth is required, which would allow calibration of the x-axis (angle A_{CG}) in Figure 3b. Included in this study are two modern animals, one from the Chillingham Wild White Cattle herd (CHIL1), the other a Dexter reared for beef (KAR). Unfortunately, the date of birth of the Chillingham animal is not known. The date of birth of the Dexter is known (8th February 2010) but this animal may not prove to be the ideal control animal because he moved to a location 10 km from his birth place when he was 3½ months old. As a result, he had access to a variety of water sources. At the first location, drinking water consisted mainly of collected rainwater and ditch water, while at the second, water was available from a stream and from a borehole. The $\delta^{18}O$ value of the borehole water may not vary appreciably with season. Despite this, the $\delta^{18}O$ profile for the first molar enamel (Fig. 2a) follows a typical sinusoidal shape, although there is a possibility of some modification by the borehole water since the enamel was still mineralizing after the move to the second location. Angle A_{CG} for the Dexter has been calculated to be -27° and is shown in Figure 3b. An angle of -27° might suggest simplistically that the completion of rumen functionality occurred in early summer, implying birth in early spring rather than February (Fig. 2a). However, the process and duration of enamel mineralization causes a temporal shift between the input and the recorded signals that

depends on the shape of the input pattern, i.e. the sinusoidal profile of $\delta^{18}O$ produced by gradual seasonal change is shifted by a different amount to the step change in $\delta^{13}C$ gradient resulting from the development of the rumen. Consequently, an angle of -27° is approximately as expected for a February birth. Most of the animals included in this study lie between -27° (KAR) and 91° (MH138), a range of 118° which represents (118/360) x 12 months = 3.9 months. If the $\delta^{18}O$ profile of the Dexter (KAR) is truly seasonal and method 2 is a valid approach to determining cattle birth seasonality, then these animals were probably born during late winter, spring and early summer. For a random selection of animals from different sites and periods, it seems reasonable that the highest density of births would have coincided with the period of maximum grass growth.

CONCLUSIONS

This study has introduced a possible new approach to determine cattle birth seasonality that utilises both carbon and oxygen isotope ratio measurements of cattle first molar enamel (method 2). The technique is based on the proposition that a change in gradient observed in many first molar $\delta^{13}C$ profiles is directly related to rumen development and methanogenesis and is therefore indirectly related to birth. This multiple-isotope approach, using both $\delta^{13}C$ and $\delta^{18}O$ profiles, has the advantage that prediction of cattle birth seasonality using method 2 should be unaffected by variability in the timing and rate of tooth crown formation. Initial results suggest that method 2 may produce more accurate estimates of cattle birth seasonality than method 1, which is based on $\delta^{18}O$ maxima and minima present in second and third molar profiles. Variability in crown formation appears to be more pronounced for third molars which could lead to inaccurate predictions of cattle birth seasonality using method 1 and erroneous conclusions regarding cattle husbandry and economic goals.

However, method 2 is still at an early stage of development and requires much more extensive testing both to verify that the patterning observed in first molar $\delta^{13}C$ profiles is indeed a result of rumen development and methanogenesis, and to further investigate and evaluate the sources of uncertainty associated with methods 1 and 2. For this purpose, the analysis of molars from modern animals with known histories would be particularly beneficial. The use of modern material would also be invaluable in the determination of season of birth in addition to birth seasonality.

ACKNOWLEDGEMENTS

The authors would like to thank the British Museum and Tankerness House Museum, Orkney, for permission to sample cattle molars in their collections, particularly Gillian Varndell and Marianne Eve (British Museum), Linda Aiano (Tankerness House Museum) and Dr Ingrid Mainland (Orkney College UHI) for facilitating the sampling. Thanks also to Chris Leyland (Chillingham Park Manager) and Professor Stephen Hall (University of Lincoln) for provision of Chillingham cattle teeth, Louisa Gidney (Durham University) for provision of modern Dexter teeth and Dr Maura Pellegrini (Oxford University) for providing an enamel laboratory standard. We are very grateful to Dr Marie Balasse and Dr Antoine Zazzo (CNRS/MNHN) for their invaluable comments and suggestions regarding earlier versions of the manuscript. This study was funded through an AHRC Studentship awarded to Jacqueline Towers.

REFERENCES

Anderson, K. L., Nagaraja, T. G., Morrill, J. L., Avery, T. B., Galitzer, S. J., and Boyer, J. E., 1987, Ruminal microbial development in conventionally or early-weaned calves, *Journal of Animal Science*, **64**, 1215-26.

Balasse, M., 2002, Reconstructing dietary and environmental history from enamel isotopic analysis: time resolution of intra-tooth sequential sampling, *International Journal of Osteoarchaeology*, **12**, 155-65.

Balasse, M., and Tresset, A., 2007, Environmental constraints on the reproductive activity of domestic sheep and cattle: what latitude for the herder? *Anthropozoologica*, **42**(2), 71-88.

Balasse, M., Smith, A. B., Ambrose, S. H., and Leigh, S. R., 2003, Determining sheep birth seasonality by analysis of tooth enamel oxygen isotope ratios: the Late Stone Age site of Kasteelberg (South Africa), *Journal of Archaeological Science*, **30**, 205-15.

Balasse, M., Obein, G., Ughetto-Monfrin, J., and Mainland, I., 2012a, Investigating seasonality and season of birth in past herds: a reference set of sheep enamel stable oxygen isotope ratios, *Archaeometry*, **54**, 349-68.

Balasse, M., Boury, L., Ughetto-Monfrin, J., and Tresset, A., 2012b, Stable isotope insights ($\delta^{18}O$, $\delta^{13}C$) into cattle and sheep husbandry at Bercy (Paris, France, 4th millennium BC): birth seasonality and winter leaf foddering, *Environmental Archaeology*, **17**, 29-44.

Berendsen, H. J. C., 2011, *A student's guide to data and error analysis*, Cambridge University Press, Cambridge.

Blaise, E., and Balasse, M., 2011, Seasonality and season of birth of modern and late Neolithic sheep from south-eastern France using tooth enamel $\delta^{18}O$ analysis, *Journal of Archaeological Science*, **38**, 3085-93.

Brown, W. A. B., Christofferson, P. V., Massler, M., and Weiss, M. B., 1960, Postnatal tooth development in cattle, *American Journal of Veterinary Research*, **21**(80), 7-34.

Bryant, M. P., Small, N., Bouma, C., and Robinson, I., 1958, Studies of the composition of the ruminal flora and fauna of young calves, *Journal of Dairy Science*, **41**, 1747-67.

Camin, F., Perini, M., Colombari, G., Bontempo, L., and Versini, G., 2008, Influence of dietary composition on the carbon, nitrogen, oxygen and hydrogen stable isotope ratios of milk, *Rapid Communications in Mass Spectrometry*, **22**, 1690-6.

Cerling, T. E., and Harris, J. M., 1999, Carbon isotope fractionation between diet and bioapatite in ungulate mammals and implications for ecological and palaeoecological studies, *Oecologia*, **120**, 347-63.

Dansgaard, W., 1964, Stable isotopes in precipitation, *Tellus*, **16**, 436-68.

Darling, W. G., and Talbot, J. C., 2003, The O & H stable isotopic composition of fresh waters in the British Isles. 1. Rainfall, *Hydrology and Earth System Sciences*, **7**, 163-81.

Davis, G. W., 2010, *The fate of neonate calves. A discussion of the bovine infant health implications of dairying, using archaeozoological studies of six Orcadian contexts*, PhD thesis, Division of Archaeological, Geographical and Environmental Sciences, University of Bradford.

Deutsch, D., El-Attar, I., Robinson, C., and Weatherell, J. A., 1979, Rate and timing of enamel development in the deciduous bovine incisor, *Archives of Oral Biology*, **24**, 407-13.

Fricke, H. C., and O'Neil, J. R., 1996, Inter- and intra-tooth variation in the oxygen isotope composition of mammalian tooth enamel phosphate: implications for palaeoclimatological and palaeobiological research, *Palaeogeography, Palaeoclimatology, Palaeoecology*, **126**, 91-9.

Fricke, H. C., Clyde, W. C., and O'Neil, J. R., 1998, Intra-tooth variations in $\delta^{18}O$ (PO_4) of mammalian tooth enamel as a record of seasonal variations in continental climate variables, *Geochimica et Cosmochimica Acta*, **62**, 1839-50.

Godfrey, N. W., 1961a, The functional development of the calf. I. Growth of the stomach of the calf, *Journal of Agricultural Science*, **57**, 173-5.

Godfrey, N. W., 1961b, The functional development of the calf. II. Development of rumen function in the calf, *Journal of Agricultural Science*, **57**, 177-83.

Grant, A., 1982, The use of tooth wear as a guide to the age of domestic ungulates, in *Ageing and sexing animal bones from archaeological sites* (eds. B. Wilson, C. Grigson and S. Payne), 91-108, British Archaeological Reports British Series 109, Oxford.

Hall, S. J. G., 1989, The white herd of Chillingham, *Journal of the Royal Agricultural Society of England*, **150**, 112-9.

Hedges, R. E. M., 2003, On bone collagen – apatite-carbonate isotopic relationships, *International Journal of Osteoarchaeology*, **13**, 66-79.

Henton, E., Meier-Augenstein, W., and Kemp, H.F., 2010, The use of oxygen isotopes in sheep molars to investigate past herding practices at the Neolithic settlement of Çatalhöyük, central Anatolia, *Archaeometry*, **52**, 429-49.

Hillson, S., 1996, *Dental anthropology*, Cambridge University Press, Cambridge.

Hillson, S., 2005, *Teeth*, 2nd ed., Cambridge University Press, Cambridge.

Hoppe, K. A., Stover, S. M., Pascoe, J. R., and Amundson, R., 2004, Tooth enamel biomineralization in extant horses: implications for isotopic microsampling, *Palaeogeography, Palaeoclimatology, Palaeoecology*, **206**, 355-65.

Hunter, J., 2007, *Investigations in Sanday, Orkney. Volume 1: excavations at Pool, Sanday. A multi-period settlement from Neolithic to Late Norse times*, The Orcadian Ltd/Historic Scotland, Kirkwall.

Jones, G. G., 2007, Variations of mandibular tooth accessory pillars, and metrical and morphological differences between M1 and M2, in the cattle associated with the chariot burial, appendix 11, in *The archaeology of the A1 (M) Darrington to Dishforth DBFO road scheme* (eds. F. Brown, C. Howard-Davis, M. Brennand, A. Boyle, T. Evans, S. O'Connor, A. Spence, R. Heawood, and A. Lupton), 618-25, Oxford Archaeology North, Lancaster.

Jordana, X., and Köhler M., 2011, Enamel microstructure in the fossil bovid *Myotragus balearicus* (Majorca, Spain): implications for life-history evolution of dwarf mammals in insular ecosystems, *Palaeogeography, Palaeoclimatology, Palaeoecology*, **300**, 59-66.

Kierdorf, H., Witzel, C., Upex, B., Dobney, K., and Kierdorf, U., 2012, Enamel hypoplasia in molars of sheep and goats, and its relationship to the pattern of tooth crown growth, *Journal of Anatomy*, **220**, 484-95.

King, J. O. L., 1978, *An introduction to animal husbandry*, Blackwell Scientific Publications, Oxford.

Kohn, M. J., 2004, Comment: Tooth enamel mineralization in ungulates: implications for recovering a primary isotopic time-series, by B. H. Passey and T. E. Cerling (2002), *Geochimica et Cosmochimica Acta*, **68**, 403-5.

Legge, A. J., 1992, *Excavations at Grimes Graves, Norfolk 1972-1976. Fascicule 4: animals, environment and the Bronze Age economy*, British Museum Press, London.

Lengemann, F. W., and Allen, N. N., 1959, Development of rumen function in the dairy calf. II. Effect of diet upon characteristics of the rumen flora and fauna of young calves, *Journal of Dairy Science*, **42**, 1171-81.

Lin, G. P., Rau, Y. H., Chen, Y. F., Chou, C. C., and Fu, W. G., 2003, Measurements of δD and $\delta^{18}O$ stable isotope ratios in milk, *Journal of Food Science*, **68**, 2192-5.

Longinelli, A., 1984, Oxygen isotopes in mammal bone phosphate: a new tool for paleohydrological and paleoclimatological research? *Geochimica et Cosmochimica Acta*, **48**, 385-90.

Luz, B., and Kolodny, Y., 1985, Oxygen isotope variations in phosphate of biogenic apatites, IV. Mammal teeth and bones, *Earth and Planetary Science Letters*, **75**, 29-36.

Luz, B., Kolodny, Y., and Horowitz, M., 1984, Fractionation of oxygen isotopes between mammalian bone-phosphate and environmental drinking water, *Geochimica et Cosmochimica Acta*, **48**, 1689-93.

McDonald, P., Edwards, R. A., and Greenhalgh, J. F. D., 1988, *Animal nutrition*, 4th edn, Longman Scientific & Technical, Harlow.

Mercer, R. J., 1981, *Grimes Graves, Norfolk. Excavations 1971-72: volume I*, Department of the Environment Archaeological Reports No 11, HMSO, London.

Metges, C., Kempe, K., and Schmidt, H-L, 1990, Dependence of the carbon-isotope contents of breath carbon dioxide, milk, serum and rumen fermentation products on the $\delta^{13}C$ value of food in dairy cows, *British Journal of Nutrition*, **63**, 187-96.

Montgomery, J., Evans, J. A., and Horstwood, M. S. A., 2010, Evidence for long-term averaging of strontium in bovine enamel using TIMS and LA-MC-ICP-MS strontium isotope intra-molar profiles, *Environmental Archaeology*, **15**: 32-42.

Passey, B. H., and Cerling, T. E., 2002, Tooth enamel mineralization in ungulates: implications for recovering a primary isotopic time-series, *Geochimica et Cosmochimica Acta*, **66**, 3225-34.

Passey, B. H., Robinson, T. F., Ayliffe, L. K., Cerling, T. E., Sponheimer, M., Dearing, M. D., Roeder, B. L., and Ehleringer, J. R., 2005, Carbon isotope fractionation between diet, breath CO_2, and bioapatite in different mammals, *Journal of Archaeological Science*, **32**, 1459-70.

Renou, J-P., Deponge, C., Gachon, P., Bonnefoy, J-C., Coulon, J-B., Garel, J-P., Vérité, R., and Ritz, P., 2004, Characterization of animal products according to geographic origin and feeding diet using nuclear magnetic resonance and isotope ratio mass spectrometry: cow milk, *Food Chemistry*, **85**, 63-6.

Robinson, C., Kirkham, J., Brookes, S. J., Bonass, W. A., and Shore, R. C., 1995, The chemistry of enamel development, *International Journal of Developmental Biology*, **39**, 145-52.

Rust F., 1981, Ruminant methane $\delta(^{13}C/^{12}C)$ values: relation to atmospheric methane, *Science*, **211**, 1044-6.

Schulze, E., Lohmeyer, S., and Giese, W., 1997, Determination of $^{13}C/^{12}C$ ratios in rumen produced methane and CO_2 of cows, sheep, and camels, *Isotopes in Environmental and Health Studies*, **33**, 75-9.

Sharp, Z., 2007, *Principles of stable isotope geochemistry*, Pearson Educational, Upper Saddle River, New Jersey.

Soana, S., Bertoni, G., Gnudi, G., and Botti, P., 1997, Anatomo-radiographic study of prenatal development of bovine fetal teeth, *Anatomia, Histologia, Embryologia*, **26**, 107-13.

Sponheimer, M., 1999, *Isotopic ecology of the Makapansgat Limeworks fauna*, PhD thesis, Rutgers University, New Jersey.

Stevens, R.E., Balasse, M., and O'Connell, T. C., 2011, Intra-tooth oxygen isotope variation in a known population of red deer: implications for past climate and seasonality reconstructions, *Palaeogeography, Palaeoclimatology, Palaeoecology*, **301**, 64-74.

Suga, S., 1982, Progressive mineralization pattern of developing enamel during the maturation stage, *Journal of Dental Research*, **61**, 1532-42.

Suga, S., Ohno, S., Misu, M., and Kondo, K., 1979, Progressive mineralization pattern of bovine developing enamel, *Japanese Journal of Oral Biology*, **21**, 117-39.

Sullivan, C. H., and Krueger, H. W., 1981, Carbon isotope analysis of separate chemical phases in modern and fossil bone, *Nature*, **292**, 333-5.

Swanson, E. W., and Harris, J. D., 1958, Development of rumination in the young calf, *Journal of Dairy Science*, **41**, 1768-76.

Tafforeau, P., Bentaleb, I., Jaeger, J-J., and Martin, C., 2007, Nature of laminations and mineralization in rhinoceros enamel using histology and X-ray synchrotron microtomography: potential implications for palaeoenvironmental isotopic studies, *Palaeogeography, Palaeoclimatology, Palaeoecology*, **246**, 206-27.

Towers, J., Jay, M., Mainland, I., Nehlich, O., and Montgomery, J., 2011, A calf for all seasons? The potential of stable isotope analysis to investigate prehistoric husbandry practices, *Journal of Archaeological Science*, **38**, 1858-68.

Zazzo, A., Balasse, M., and Patterson, W.P., 2005, High-resolution $\delta^{13}C$ intratooth profiles in bovine enamel: implications for mineralization pattern and isotopic attenuation, *Geochimica et Cosmochimica Acta*, **69**, 3631-42.

Zazzo, A., Balasse, M., Passey, B. H., Moloney, A. P., Monahan, F. J., and Schmidt, O., 2010, The isotope record of short- and long-term dietary changes in sheep tooth enamel:

implications for quantitative reconstruction of paleodiets, *Geochimica et Cosmochimica Acta*, **74**, 3571-86.

Zazzo, A., Bendrey, R., Vella, D., Moloney, A. P., Monahan, F. J., and Schmidt, O., 2012, A refined sampling strategy for intra-tooth stable isotope analysis of mammalian enamel, *Geochimica et Cosmochimica Acta*, **84**, 1-13.

TABLES

Table 1 Chronology of development of mandibular cattle molars (data from Brown et al. 1960). * Foetal age of 140 days (Soana et al. 1997), equivalent to approximately 4.7 months before birth

Development	First molar (age in months)	Second molar (age in months)	Third molar (age in months)
Crown formation starts	In utero*	1	9-10
Crown formation complete	2-3	12-13	23-24

Table 2 Oxygen and carbon isotope ratios of cattle molar enamel. PL = Pool, GG = Grimes Graves, MH = Mine Howe, CHIL = Chillingham and KAR = dexter from County Durham. Mandibular 1st, 2nd and 3rd molars are designated M_1, M_2 and M_3. Mandibular 4th deciduous premolars are designated dP_4. LM = lingual mesial, LD = lingual distal, LC = lingual central, BM = buccal mesial. Wear stages after Grant (1982)

Sample No.	Distance from cervix (mm)	$\delta^{18}O_{VSMOW}$ normalised (‰)	$\delta^{13}C_{VPDB}$ normalised (‰)	Sample No.	Distance from cervix (mm)	$\delta^{18}O_{VSMOW}$ normalised (‰)	$\delta^{13}C_{VPDB}$ normalised (‰)	Sample No.	Distance from cervix (mm)	$\delta^{18}O_{VSMOW}$ normalised (‰)	$\delta^{13}C_{VPDB}$ normalised (‰)
PL0278 (M_1), LM, wear stage j, cusp to cervix 31.5 mm				PL0278 (M_2), LM, wear stage e/f, cusp to cervix 43.0 mm				PL0278 (M_3), LM, wear stage a, cusp to cervix 49.0 mm			
1	28.5	26.4	-14.5	1	39.0	23.8	-11.4	1	45.0	25.1	-11.3
2	24.5	26.2	-14.0	2	35.0	23.8	-11.2	2	41.0	24.7	-11.5
3	21.0	26.4	-13.6	3	31.0	24.0	-11.1	3	37.0	24.2	-11.7
4	17.0	26.5	-12.9	4	27.5	24.1	-11.2	4	33.0	23.9	-11.8
5	13.5	25.8	-12.4	5	24.0	24.4	-11.2	5	29.5	24.1	-11.8
6	9.5	25.3	-11.9	6	20.5	25.3	-11.3	6	25.5	24.5	-11.9
7	5.5	25.1	-11.6	7	16.5	25.8	-11.5	7	22.0	24.6	-12.0
8	2.5	24.7	-11.4	8	12.5	26.3	-11.5	8	19.0	25.0	-12.0
				9	8.5	26.0	-11.5	9	16.0	25.6	-12.0
				10	4.5	25.1	-11.3	10	13.0	25.9	-11.9
								11	10.0	26.3	-11.6
PL0330 (M_1), LM, wear stage g, cusp to cervix 35.5 mm				PL0330 (M_2), LD, cusp damaged				PL0330 (M_3), LC, wear stage a/b, cusp to cervix 51.0 mm			
1	33.0	24.5	-13.6	1	34.0	23.7	-11.8	1	45.0	25.1	-11.3
2	28.5	25.5	-13.6	2	28.0	24.0	-11.9	2	39.5	24.4	-11.3
3	24.5	26.1	-13.4	3	24.5	24.6	-11.9	3	33.5	24.2	-11.4
4	21.5	26.4	-13.1	4	21.0	25.1	-11.8	4	28.0	24.1	-11.6
5	15.5	26.5	-12.5	5	17.5	25.5	-11.9	5	22.0	24.3	-11.9

6	12.0	27.0	-12.4	6	13.5	25.5	-12.1	6	16.5	25.3	-12.2
7	9.0	26.5	-12.4	7	10.0	26.0	-12.0	7	11.0	26.0	-12.3
8	6.0	26.1	-12.1	8	6.5	26.3	-11.8	8	6.0	26.0	-12.0
9	2.5	25.4	-12.1	9	3.0	25.6	-11.5				

PL0339 (M_1), LM, wear stage h, cusp to cervix 33.5 mm

1	27.0	23.5	-14.5
2	23.0	23.8	-13.7
3	18.5	24.2	-13.3
4	14.5	24.7	-13.0
5	11.0	25.6	-13.1
6	6.5	26.5	-13.0
7	3.5	27.1	-12.8

PL0339 (M_2), LM, wear stage f, cusp to cervix 44.0 mm

1	36.0	26.8	-12.0
2	31.5	26.8	-11.8
3	27.0	26.0	-11.7
4	22.5	24.9	-11.9
5	18.0	24.5	-11.9
6	14.0	24.0	-12.2
7	9.5	24.1	-12.3
8	6.0	23.9	-12.5
9	2.5	24.5	-12.6

PL0344 (M_1), LD, wear stage g, cusp to cervix 35.0 mm

1	30.0	24.1	-14.7
2	26.0	25.0	-14.5
3	22.5	25.7	-14.4
4	18.5	26.3	-14.4
5	15.0	27.4	-13.9
6	11.5	27.3	-13.2
7	6.5	26.8	-12.5
8	3.0	26.4	-12.4

PL0344 (M_2), LD, wear stage f, cusp to cervix 44.0 mm

1	41.0	24.9	-12.6
2	38.0	24.5	-12.3
3	35.0	24.1	-12.3
4	32.0	23.9	-12.4
5	29.0	23.9	-12.5
6	26.0	23.7	-12.4
7	23.0	23.5	-12.4
8	20.5	23.3	-12.2
9	17.0	23.3	-12.2
10	13.5	24.1	-12.2
11	10.5	24.5	-12.2
12	7.5	24.9	-12.2
13	4.0	26.0	-12.2

PL0344 (M_3), LC, wear stage b, cusp to cervix 48.0 mm

1	46.5	25.7	-12.0
2	43.5	25.5	-12.0
3	40.5	25.4	-11.8
4	37.0	24.8	-11.7
5	34.0	24.6	-11.7
6	31.0	24.4	-11.8
7	28.0	24.1	-11.9
8	25.0	24.0	-12.0
9	22.0	23.7	-12.1
10	19.0	23.4	-12.1
11	16.5	23.6	-12.3
12	13.5	23.8	-12.4
13	10.5	24.1	-12.5
14	7.5	24.6	-12.4
15	4.0	25.1	-12.1

PL0386 (M_1), LM, wear stage g, cusp to cervix 39.0 mm

1	36.0	26.3	-15.3
2	32.5	26.3	-15.0
3	29.5	26.6	-14.6
4	26.0	26.4	-14.3
5	22.5	26.0	-13.8
6	19.0	25.8	-13.3
7	15.5	25.3	-13.0
8	12.5	24.5	-12.7
9	9.0	23.9	-12.3
10	6.0	23.6	-12.0
11	3.0	23.5	-11.9

PL0386 (M_2), LM, wear stage f, cusp to cervix 51.5 mm

1	49.5	23.9	-11.9
2	47.0	23.8	-11.7
3	44.0	23.8	-11.6
4	41.0	24.2	-11.5
5	38.0	24.5	-11.6
6	34.5	25.1	-11.5
7	31.0	26.1	-11.6
8	28.0	26.6	-11.7
9	25.5	26.7	-11.8
10	22.0	26.9	-11.7
11	19.0	26.8	-11.6
12	16.0	26.3	-11.5
13	13.5	25.7	-11.5
14	10.5	25.3	-11.4
15	7.5	24.7	-11.3
16	4.5	24.5	-11.2

PL0386 (M_3), LM, wear stage a/b, cusp to cervix 57.5 mm

1	55.0	25.3	-11.1
2	52.0	24.6	-11.2
3	49.0	24.3	-11.0
4	46.5	24.1	-11.2
5	43.5	23.7	-11.3
6	40.0	24.0	-11.4
7	36.5	24.1	-11.6
8	33.0	24.1	-11.7
9	29.0	24.7	-11.8
10	25.5	25.2	-11.9
11	22.5	25.5	-12.0
12	19.5	25.7	-12.0
13	16.5	25.6	-12.0
14	13.5	25.6	-11.9
15	10.5	25.2	-11.8
16	7.0	25.2	-11.6
17	3.5	25.1	-11.6

GG839 (M_1), LM, wear stage k, cusp to cervix 29.0 mm

1	25.0	23.6	-15.7
2	21.0	24.2	-15.4
3	17.5	25.4	-15.2
4	13.0	26.0	-14.7
5	10.0	27.2	-14.3
6	6.5	27.4	-14.0
7	3.0	27.5	-13.8

GG839 (M_2), LM, wear stage g, cusp to cervix 44.5 mm

1	39.0	26.6	-13.7
2	34.5	26.2	-13.6
3	30.5	25.2	-13.7
4	27.5	24.5	-13.5
5	24.0	24.0	-13.6
6	20.0	23.8	-13.6
7	16.5	23.7	-13.6
8	12.5	23.9	-13.7
9	9.0	24.1	-13.7
10	5.0	24.8	-13.5
11	2.5	26.2	-13.2

GG839 (M_3), LM, wear stage d, cusp to cervix 49.5 mm

1	45.0	24.9	-13.0
2	41.0	25.6	-12.7
3	37.5	26.2	-12.4
4	34.0	26.5	-12.1
5	30.5	26.3	-11.6
6	27.5	25.5	-11.6
7	24.0	24.9	-11.6
8	20.5	24.3	-11.6
9	17.0	23.9	-11.6
10	13.5	24.0	-11.6
11	10.0	23.6	-11.8
12	6.5	23.2	-11.8
13	3.0	23.5	-11.8

GG743 (M_1), LM, wear stage k/l, cusp to cervix 32.5 mm

1	29.0	26.6	-15.1
2	25.0	26.3	-14.8
3	21.5	26.1	-14.3
4	17.0	25.4	-14.1
5	13.5	25.4	-14.1
6	10.0	24.3	-13.8
7	6.0	23.8	-13.9
8	2.5	23.6	-13.8

GG743 (M_2), LM, wear stage g, cusp to cervix 45.5 mm

1	38.5	23.8	-13.6
2	34.0	24.0	-13.3
3	30.0	24.5	-13.4
4	26.5	24.9	-13.1
5	23.0	25.5	-12.8
6	19.0	26.1	-12.4
7	15.5	25.7	-12.1
8	12.0	25.6	-11.8
9	8.5	25.2	-11.9
10	2.5	24.4	-12.2

GG743 (M_3), LM, wear stage e/f, cusp to cervix 51.0 mm

1	46.0	23.9	-12.3
2	41.5	24.1	-12.4
3	37.5	23.4	-12.7
4	33.5	23.3	-13.0
5	29.5	23.5	-13.3
6	26.5	23.9	-13.5
7	19.0	24.7	-13.3
8	15.5	25.1	-13.1
9	12.0	25.3	-12.6
10	8.0	25.3	-12.2
11	4.0	25.1	-12.2

GG614 (M_1), LM, wear stage j/h, cusp to cervix 37.0 mm

1	34.5	26.8	-16.1
2	30.5	27.2	-15.5
3	27.0	27.3	-14.8
4	23.5	27.1	-14.2
5	20.0	26.8	-13.8
6	16.5	26.2	-13.5
7	13.0	25.6	-13.5
8	9.5	25.0	-13.4
9	6.5	24.8	-13.5
10	3.5	24.4	-13.4

GG614 (M_2), LM, wear stage f, cusp to cervix 48.5 mm

1	42.5	24.0	-13.6
2	37.5	23.6	-13.6
3	33.0	23.7	-13.6
4	28.5	24.1	-13.4
5	23.5	25.0	-13.5
6	19.5	25.9	-13.2
7	15.5	26.7	-12.9
8	11.5	27.0	-12.7
9	7.0	26.4	-12.1
10	3.5	26.1	-12.0

GGT10 (M_1), LM, wear stage k/l, cusp to cervix 28.5 mm

1	25.0	26.4	-15.9
2	21.0	26.4	-15.3
3	17.0	26.4	-14.5
4	13.5	26.0	-13.7

GGT10 (M_2), LM, wear stage g, cusp to cervix 41.0 mm

1	35.0	24.0	-13.1
2	31.0	23.7	-13.2
3	26.5	23.8	-13.2
4	22.5	24.2	-13.1

GGT10 (M_3), LM, wear stage f, cusp to cervix 49.0 mm

1	42.0	24.9	-12.8
2	38.0	24.5	-12.8
3	34.0	24.0	-12.9
4	30.5	23.5	-13.0

5	10.0	25.6	-13.5	5	19.0	24.8	-13.1	5	26.5	23.4	-13.0
6	5.5	25.0	-13.4	6	15.5	25.6	-12.9	6	23.0	23.3	-12.8
7	2.5	24.9	-13.2	7	12.5	26.3	-12.8	7	20.0	23.3	-12.8
				8	8.5	26.5	-12.7	8	16.5	23.7	-12.6
				9	5.0	26.2	-12.5	9	13.0	24.8	-12.3
				10	2.0	25.7	-12.6	10	10.0	25.9	-11.8
								11	6.5	26.9	-11.3
								12	3.5	27.2	-11.3
GG120 (M_1), LM, wear stage f, cusp to cervix 39.5 mm				GG120 (M_2), LM, wear stage a/b, cusp to cervix 50.0 mm							
1	34.5	24.9	-16.1	1	44.0	23.3	-14.2				
2	30.5	24.7	-16.5	2	40.0	23.4	-14.2				
3	27.0		-16.5	3	36.0	22.7	-14.3				
4	22.5	25.5	-16.0	4	32.5	22.8	-14.3				
5	19.0		-15.7	5	29.5	23.0	-14.4				
6	14.5	25.6	-14.4	6	26.0	23.1	-14.4				
7	11.0	25.3	-14.4	7	22.0	23.4	-14.3				
8	7.5	23.9	-14.1	8	18.0	23.9	-14.1				
9	4.0	22.5	-14.0	9	14.5	24.7	-13.8				
				10	10.5	24.6	-13.2				
				11	6.0	24.8	-12.9				
				12	3.0	24.9	-12.9				
MH138 (M_1), LM, wear stage l, cusp to cervix 23.5 mm				MH138 (M_2), LM, wear stage k, cusp to cervix 35.0 mm				MH138 (M_3), LM, wear stage f, cusp to cervix 44.5 mm			
1	22.5	26.3	-14.9	1	33.0	24.4	-12.6	1	42.5	24.8	-12.8
2	20.0	26.1	-14.2	2	30.0	24.9	-12.4	2	39.5	24.4	-12.9
3	17.0	25.5	-13.7	3	27.0	25.0	-12.2	3	36.0	24.2	-12.8
4	15.0	25.3	-13.5	4	24.0	25.4	-12.3	4	33.0	23.9	-12.9
5	12.0	25.5	-13.5	5	21.0	26.4	-12.3	5	30.0	23.6	-13.0
6	9.5	24.8	-13.3	6	18.5	26.6	-12.4	6	27.0	24.3	-12.9
7	6.5	24.8	-13.2	7	15.5	26.3	-12.3	7	24.0	24.5	-13.2
8	4.0	24.2	-13.3	8	12.5	26.3	-12.6	8	21.0	24.6	-13.0
				9	9.5	25.9	-12.6	9	18.5	25.0	-12.6

10	6.5	25.3	-12.6
11	3.5	24.9	-12.6

10	15.5	25.5	-12.4
11	12.5	25.9	-12.4
12	9.5	25.0	-12.3
13	7.0	24.8	-12.4
14	3.5	23.9	-12.5

MH0604 (M_1), LM, wear stage k, cusp to cervix 22.0 mm

1	19.0	25.6	-15.6
2	16.5	26.0	-15.3
3	13.5	26.4	-14.9
4	11.0	26.2	-14.5
5	8.0	26.6	-14.1
6	5.5	26.6	-13.7
7	3.0	26.3	-13.9

MH0604 (M_2), LM, wear stage j, cusp to cervix 32.5 mm

1	29.0	24.6	-12.7
2	26.0	24.4	-12.8
3	23.5	24.4	-12.7
4	20.5	24.1	-12.6
5	18.0	24.2	-12.6
6	15.0	24.4	-12.5
7	12.0	24.6	-12.6
8	9.0	24.7	-12.5
9	6.0	24.6	-12.6
10	3.0	25.6	-12.4

MH0604 (M_3), LM, wear stage f, cusp to cervix 45.0 mm

1	42.0	26.0	-11.9
2	38.5	26.1	-11.8
3	35.5	26.3	-11.8
4	32.5	26.0	-11.8
5	29.5	25.6	-11.7
6	27.0	25.4	-11.8
7	24.0	24.9	-11.8
8	21.0	24.4	-11.8
9	18.0	24.2	-11.9
10	15.5	23.8	-12.1
11	12.5	23.6	-12.1
12	9.5	23.5	-12.2
13	6.5	23.6	-12.3
14	3.5	23.7	-12.4

MH84 (M_1), LD, wear stage g, cusp to cervix 38.5 mm

1	34.0	24.6	-16.5
2	30.5	25.4	-16.3
3	27.0	25.9	-15.9
4	23.5	25.8	-15.2
5	20.0	25.9	-14.5
6	16.5	25.7	-13.9
7	12.5	25.6	-13.4
8	9.0	24.9	-13.3
9	5.5	24.6	-13.1

MH84 (M_2), LD, wear stage c, cusp to cervix 48.5 mm

1	46.0	23.7	-13.2
2	43.0	23.9	-12.9
3	40.0	23.9	-12.7
4	36.5	23.8	-12.6
5	33.0	23.7	-12.6
6	30.0	23.8	-12.4
7	27.0	24.3	-12.3
8	24.0	24.2	-12.3
9	20.5	24.7	-12.2
10	17.5	25.4	-12.2

				11	14.0	26.0	-12.1
				12	11.0	26.4	-12.1
				13	8.0	26.4	-12.1
				14	4.5	26.0	-12.3
CHIL1 (M_1), BM, wear stage h, cusp to cervix 30.5 mm				CHIL1 (dP_4), cusp to cervix 10.0 mm			
1	28.5	25.9	-18.1	1	8.5		-16.0
2	25.0	26.0	-17.5	2	6.0		-16.4
3	22.0	25.8	-17.2	3	3.5		-16.4
4	19.0	25.6	-17.0				
5	15.5	25.0	-17.1				
6	12.0	24.5	-16.9				
7	8.5	24.0	-17.0				
8	4.5	23.5	-16.9				
KAR (M_1), LM, wear stage g, cusp to cervix 38.5mm				KAR (dP_4), cusp to cervix 14.0 mm			
1	34.5	21.4	-17.7	1	11.5		-15.6
2	31.0	21.6	-18.0	2	8.0		-15.6
3	27.5	22.4	-18.1	3	4.5		-16.0
4	24.0	23.0	-18.0	4	2.0		-16.1
5	21.0	23.2	-17.8				
6	17.5	23.7	-17.5				
7	14.0	24.8	-17.0				
8	10.5	24.7	-16.6				
9	7.0	25.0	-16.5				
10	3.0	25.0	-16.3				

Table 3 Timings of minima and maxima of $\delta^{18}O$ profiles for all archaeological cattle

Animal	Predicted time after birth (months)					
	M2 $\delta^{18}O$ minimum (min 1)	$\delta^{18}O$ maximum max	M3 $\delta^{18}O$ minimum (min 2)	[max - min 1] (months)	[min 2 - max] (months)	[min 2 - min 1] (months)
PL0278	4.5	9.4	14.5	5.0	5.1	10.0
PL0330	4.9	10.5	15.3	5.6	4.8	10.4
PL0344	6.7	11.8	18.2	5.1	6.5	11.5
PL0386	2.4	7.9	13.7	5.5	5.8	11.3
GG839	8.6	14.8	21.9	6.1	7.1	13.2
GG743	3.4	9.0	15.4	5.6	6.4	12.0
GGT10	5.6	10.7	17.8	5.2	7.1	12.3
MH138	3.4	8.9	15.4	5.4	6.5	12.0
MH0604	8.0	14.0	21.2	6.0	7.2	13.2
GG614	5.1	10.2		5.1		
MH84	4.4	10.3		5.9		
PL0339	10.3					
GG120	4.9		mean =	5.5	6.3	11.8
			σ =	0.4	0.9	1.1

Table 4 Angular positions of $\delta^{18}O_{CG}$ on the $\delta^{18}O$ profile for all cattle

Animal	Angle A_{CG} (^{o})
PL0278	91
PL0330	0
PL0339	-112
PL0344	42
PL0386	161
GG839	-13
GG743	53
GG614	68
GGT10	47
GG120	12
MH138	91
MH0604	13
MH84	49
CHIL1	44
KAR	-27

FIGURES

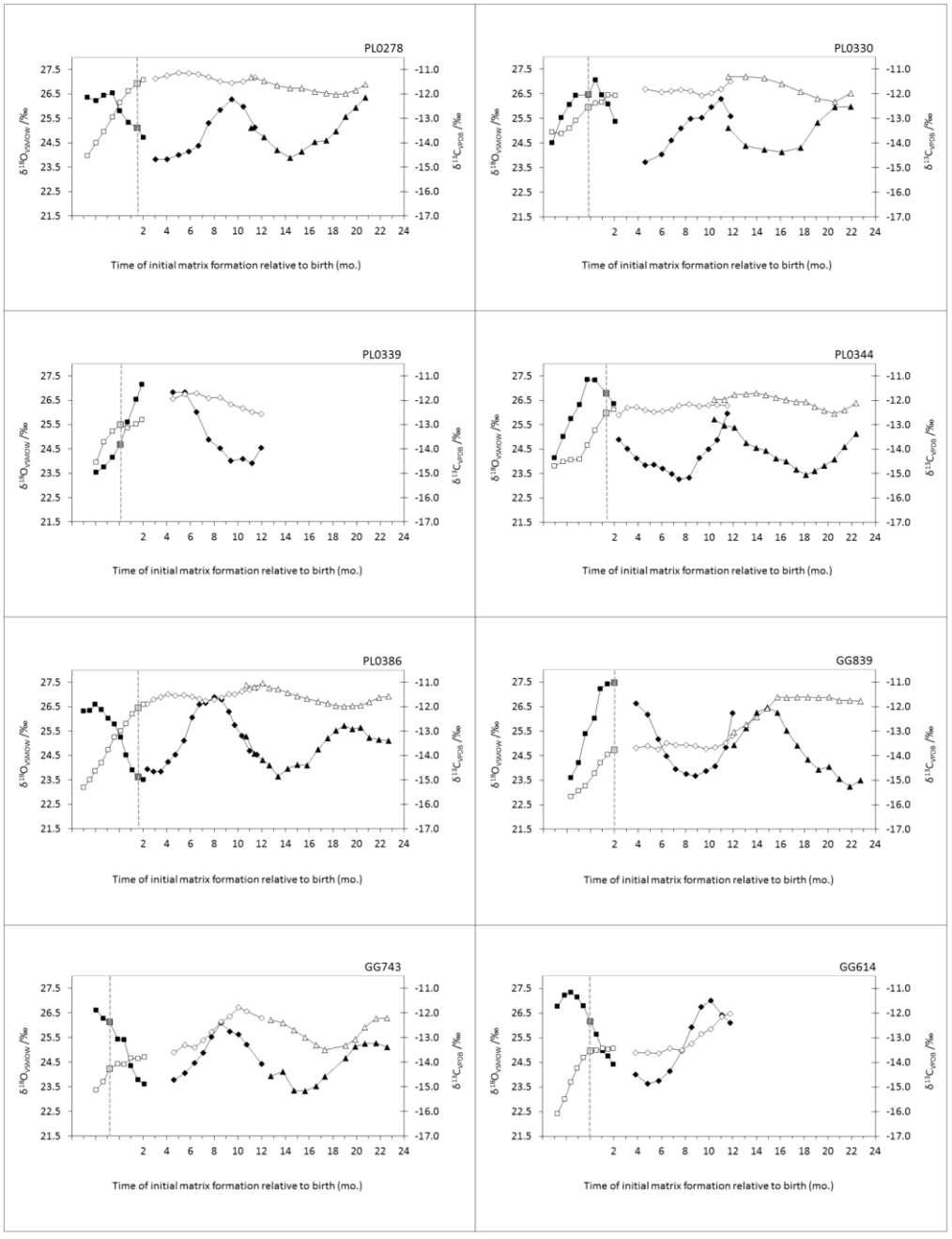
PL0278
PL0330
PL0339
PL0344
PL0386
GG839
GG743
GG614
Time of initial matrix formation relative to birth (mo.)

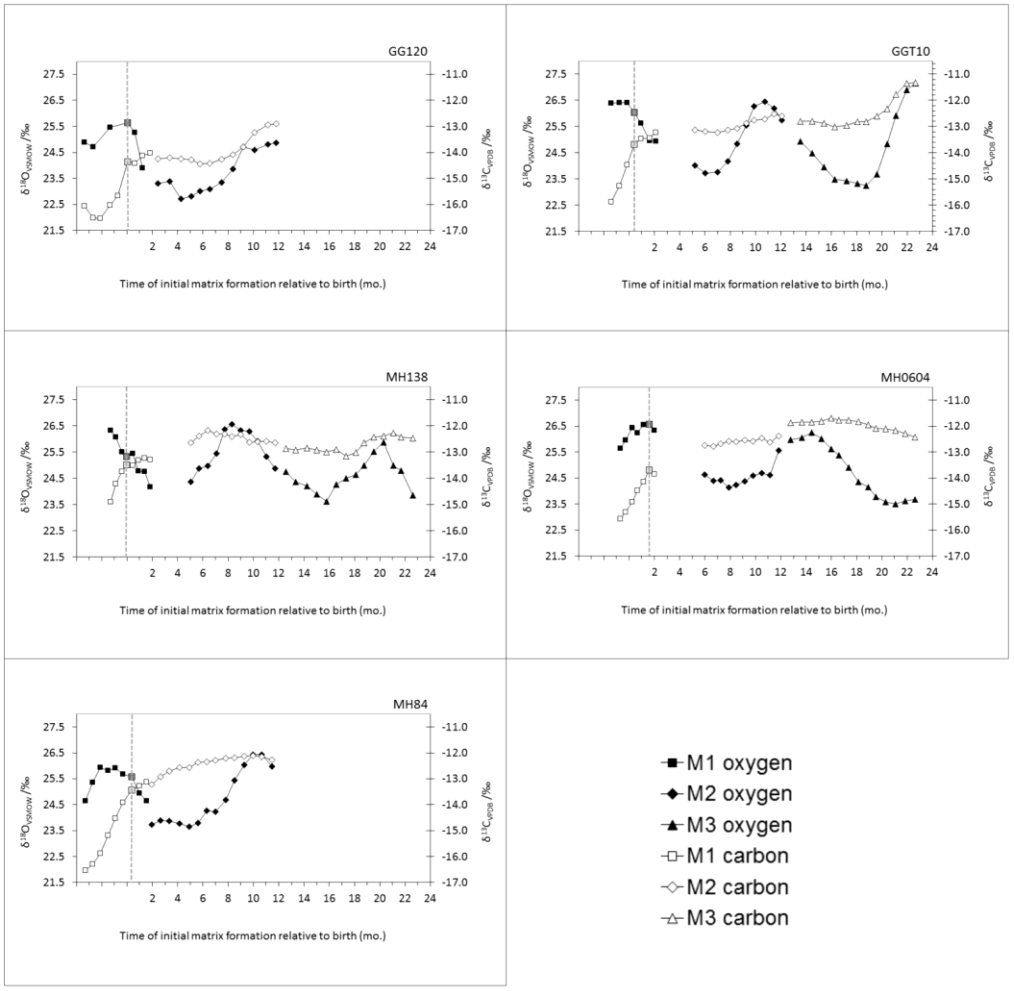

Figure 1 Combined $\delta^{18}O$ and $\delta^{13}C$ profiles for first, second and third cattle molars. Analytical error is ± 0.1‰ for $\delta^{13}C_{VPDB}$ and ± 0.2‰ for $\delta^{18}O_{VSMOW}$. The grey square symbols connected by a dashed line represent $\delta^{13}C_{CG}$ and $\delta^{18}O_{CG}$

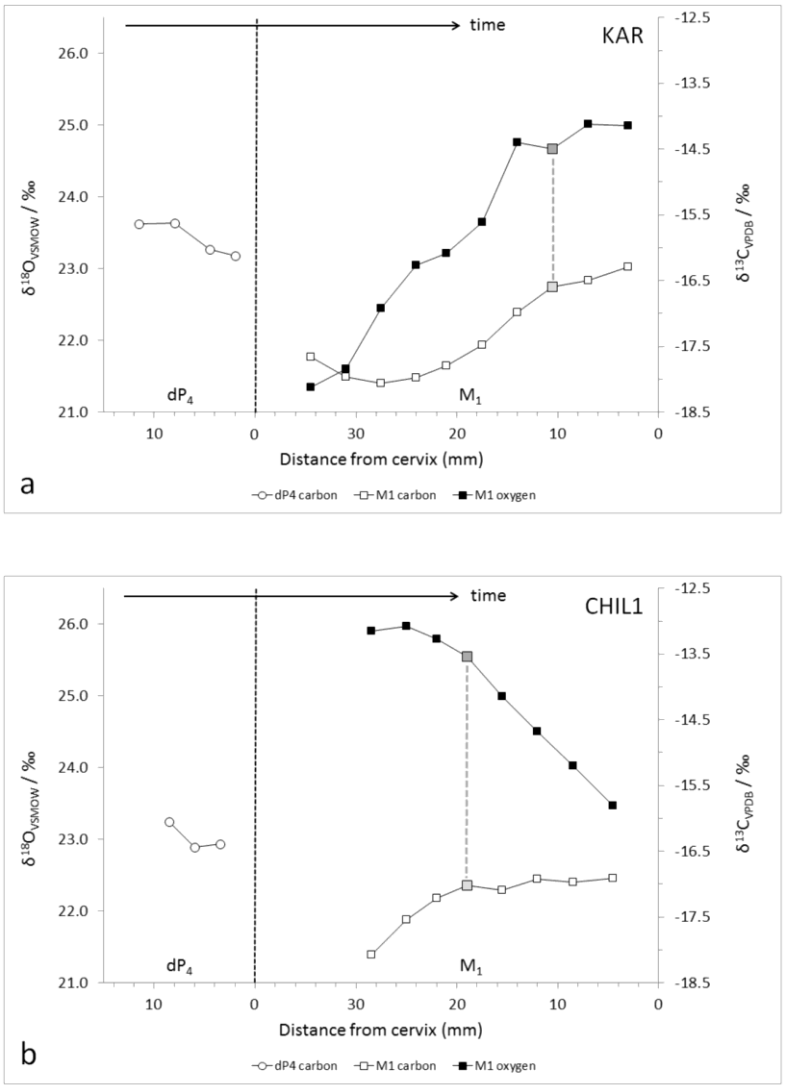

Figure 2 $\delta^{18}O$ and $\delta^{13}C$ versus distance from cervix for first molars and 4th deciduous premolars from animals KAR (a) and CHIL1 (b). The grey square symbols connected by a dashed line represent $\delta^{13}C_{CG}$ and $\delta^{18}O_{CG}$

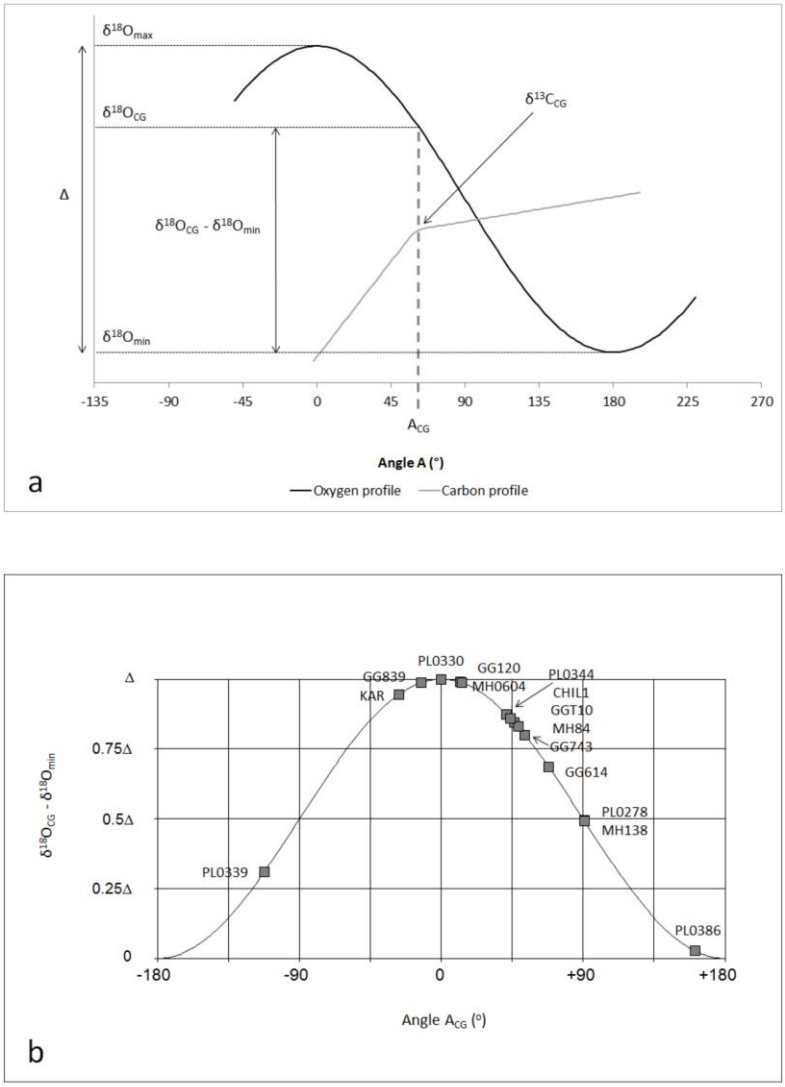

Figure 3 a) Schematic diagram showing the parameters involved in the calculation of A_{CG}; b) Angles A_{CG} for all cattle

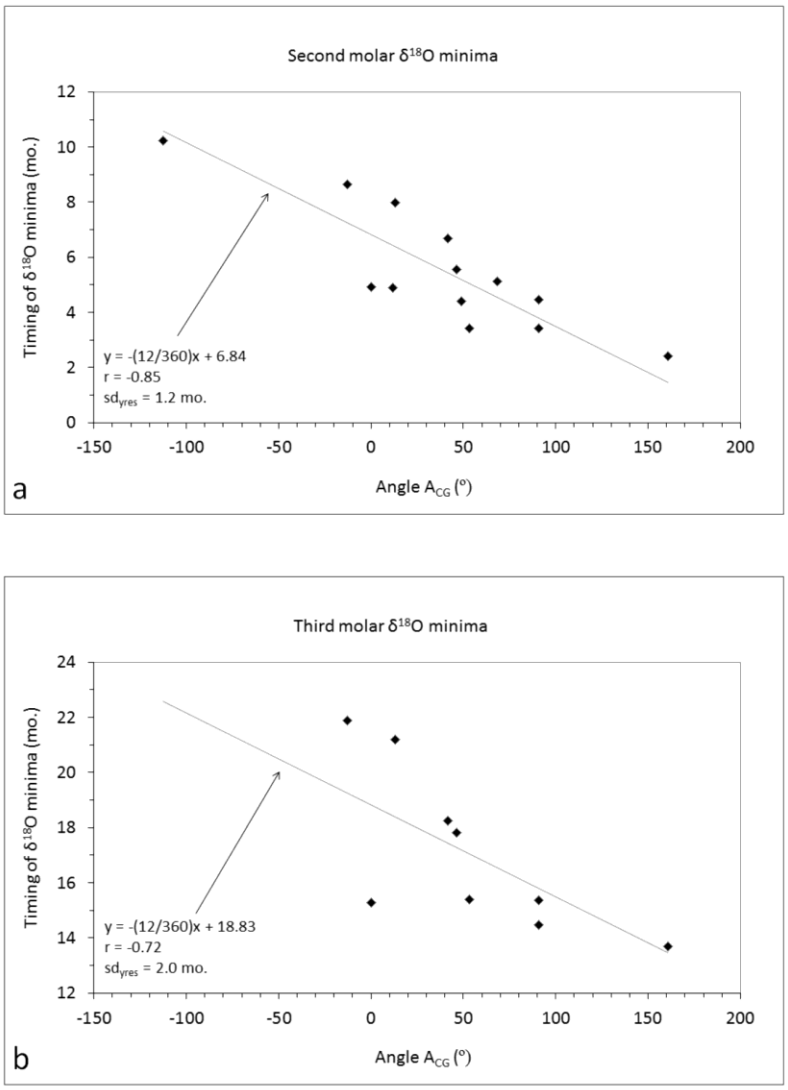

Figure 4 a) Second molar $\delta^{18}O$ minima timings versus A_{CG}; b) Third molar $\delta^{18}O$ minima timings versus A_{CG}